Preparation and properties of epitaxial $La_{0.7}Ca_{0.3}MnO_{3-\delta}$ films with reduced carrier density

2000 J. Phys.: Condens. Matter 12 7099

(http://iopscience.iop.org/0953-8984/12/31/311)

J. Phys.: Condens. Matter **12** (2000) 7099–7109. Printed in the UK PII: S0953-8984(00)11074-4

Preparation and properties of epitaxial $La_{0.7}Ca_{0.3}MnO_{3-\delta}$ films with reduced carrier density

K Dörr†, J M De Teresa†‖, K-H Müller†, D Eckert†, T Walter†, E Vlakhov†‡, K Nenkov†§ and L Schultz†

† IFW Dresden, Postfach 270016, D-01171 Dresden, Germany
‡ Institute of Solid State Physics, Bulgarian Academy of Sciences, Sofia 1784, Bulgaria
§ International Laboratory for High Magnetic Fields and Low Temperatures, 53-529 Wroclaw, Poland

E-mail: k.doerr@ifw-dresden.de

Received 17 January 2000, in final form 15 May 2000

Abstract. Epitaxial $La_{0.7}Ca_{0.3}MnO_{3-\delta}$ thin films have been grown on $LaAlO_3(100)$ substrates by magnetron sputtering. By vacuum annealing at temperatures below 600 °C, oxygen-deficient films with ferromagnetic ordering temperatures, T_C, between 130 K and 270 K have been prepared. Oxygen deficiency reduces the Mn^{4+} content, i.e. the charge carrier density of the films. Effective oxygen diffusion was observed at temperatures as low as $T = 80$ °C. Resistance, magnetization and magnetoresistance behaviours of the films are reported. Our results are consistent with a magnetically phase-separated ground state—a mixture of ferromagnetic metallic and antiferromagnetic insulating regions—of $La_{0.7}Ca_{0.3}MnO_{3-\delta}$ for an Mn^{4+} concentration below ∼20%. The electrical transport in the oxygen-deficient films, e.g. the non-monotonic temperature dependence of the resistance, the large magnetoresistance at $T < T_C$ and the low-field magnetoresistance observed for some of the investigated samples, can be explained by a percolation mechanism in the phase-separated state.

1. Introduction

The discovery of colossal magnetoresistance (CMR) in $La_{1-x}M_xMnO_3$ (M = Ca, Ba, Sr) thin films [1, 2] and its possible application in magnetoresistive devices have stimulated much interest in the family of manganites in recent years [3, 4]. Metallic conductivity and ferromagnetism have been found around $0.2 \leqslant x \leqslant 0.5$ and explained in terms of Zener's double-exchange interaction characterized by electron transfer from Mn^{3+} to Mn^{4+} ions via O 2p orbitals [5–7]. The transport properties of these compounds depend on the hole concentration (i.e. the Mn^{4+} content) and on structural parameters such as Mn–O distances and Mn–O–Mn bond angles [8]. The hole concentration may be modified by changing either the doping level x or the oxygen content $3 - \delta$. Thus, a stepwise increase of δ should allow access to the low-Mn^{4+}-concentration range of the phase diagram as long as order/disorder effects of the vacancies and modifications of the crystal structure are negligible. The equilibrium value of δ in dependence on temperature and oxygen partial pressure was established for a $La_{0.85}Sr_{0.15}MnO_{3-\delta}$ single crystal [9]. Oxygen-deficient polycrystalline bulk samples of several compounds have been investigated concerning their magnetism and

‖ Current address: Departamento de Física de la Materia Condensada, University of Zaragoza-CSIC, 50 009 Zaragoza, Spain.

0953-8984/00/317099+11$30.00

magnetoresistance [10–13]. Controlled oxygen deficiency in thin films has been achieved either by annealing as-deposited films under vacuum conditions (e.g. for $La_{0.7}Ca_{0.3}MnO_{3-\delta}$ [14] and $La_{0.7}Sr_{0.3}MnO_{3-\delta}$ [15]) or by film growth in reduced oxygen partial pressures [16]. In all cases, oxygen deficiency was found to cause a modification of magnetic and transport properties that can roughly be understood by the resulting change of the hole concentration c, $\Delta c(Mn^{4+}) = -2\delta$. That is, for ferromagnetic $La_{0.7}M_{0.3}MnO_3$, oxygen deficiency leads to (i) a decrease of the Curie temperature (T_C) and the associated metal–insulator transition temperature (T_{MI}), (ii) an increase of resistivity and (iii) a reduced magnetization of the samples. The latter had been attributed to a canted arrangement of Mn spins [7], but recent experiments [4, 11, 17–19] on Ca-doped manganites and theoretical argumentation [20–22] strongly point to a magnetic phase separation with a coexistence, at low temperatures, of ferromagnetic and antiferromagnetic regions on a nanometre scale. Experimental and theoretical support for magnetic phase separation in CMR manganites has been growing recently (for a summary see [22]). Electronic phase separation is a well known characteristic of some oxides, e.g. the cuprate superconductors [23]. For the low-doping range of Ca doped manganites, microscopic measurements such as nuclear magnetic resonance [17] and small-angle neutron scattering [4] seem to confirm the phase separation. Uehara *et al* have presented electron-microscopy images showing a mixture of ferromagnetic and charge-ordered (antiferromagnetic) sub-micron domains in Nd-substituted $La_{0.62}Ca_{0.38}MnO_3$ [19]. In such a two-phase state, electrical conduction and magnetoresistance will mainly depend on the spatial distribution of the highly conductive ferromagnetic phase and its change with an applied magnetic field (i.e. the effective electrical conductivity will be governed by some percolation mechanism).

In this study, epitaxial $La_{0.7}Ca_{0.3}MnO_{3-\delta}$ thin films with $T_C = 130$ K to 270 K, referring approximately to $\delta = -0.02$ to 0.1 or 10 to 34% of Mn^{4+}, have been prepared by magnetron sputtering and a medium-temperature vacuum annealing procedure that should not affect the microstructure (morphology) of the films. Results of magnetization and electrical resistance measurements are discussed in the framework of a magnetically phase-separated low-temperature state.

2. Experiments

Epitaxial $La_{0.7}Ca_{0.3}MnO_{3-\delta}$ thin films of a thickness of 80 ± 10 nm were grown on $LaAlO_3$ (100) single-crystalline substrates by radio frequency magnetron sputtering [24]. The grain size of the films is around 70 nm, estimated from scanning electron microscopy images of the film surface. Oxygen was removed from the films by annealing them under a constant vacuum pressure of 5×10^{-5} mbar at an annealing temperature (T_A) of $300\,^{\circ}C \leqslant T_A \leqslant 550\,^{\circ}C$ for a duration of 30 to 300 min. A definite pre-annealing state of all samples was provided by an air annealing step at 700 °C for 30 min. The resulting oxygen content should be ~3.02, as can be expected from thermochemical studies for $La_{0.7}Sr_{0.3}MnO_{3-\delta}$ published in [14]. The oxygen deficiency of each thin film could not be directly determined but we used the linear relationship between the Curie temperature and the mean Mn valency found in literature for oxygen-deficient $La_{0.7}M_{0.3}MnO_{3-\delta}$ (~7 K/0.01 Mn valency change) in the investigated Mn^{4+} concentration range [10, 11, 14]. This is expected to be a good estimate allowing us to perform a quantitative analysis. The structure of the films was investigated at room temperature by x-ray diffraction including pole-figure measurements. Low-temperature magnetic and magnetotransport properties were measured in a Lake Shore susceptometer and a SQUID

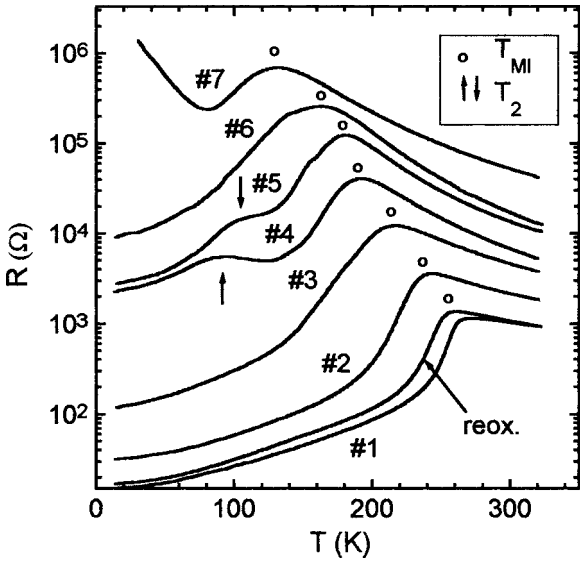

Figure 1. Temperature dependence of the resistance of $La_{0.7}Ca_{0.3}MnO_{3-\delta}$ films for $\delta(1) < \delta(2) < \delta(3) < \delta(4) < \delta(5) < \delta(6) < \delta(7) \approx 0.1$, $\delta(1) \approx -0.02$. The metal–insulator transition temperature, T_{MI}, is near the ferromagnetic ordering temperature. T_2 denotes the low-temperature peak of resistance. A curve measured after reoxidation is also shown.

magnetometer. Resistance measurements were made by the usual four-probe or by the van der Pauw technique. For measurements above room temperature, a home-made tube furnace wasused.

3. Results

X-ray θ–2θ plots show only (00n) reflections (referring to a pseudocubic lattice) for the investigated films. In-plane texture was checked to be cube-on-cube by pole-figure measurements. The out-of-plane lattice constant was found to increase with δ, from the value of 3.868 Å for sample 1 to 3.936 Å for sample 7. The (00n) reflections were somewhat broadened for the samples with large δ, e.g. the (002) peak showing a FWHM (full width at half maximum) value of 0.4° for sample 1 and 0.65° for sample 7, respectively. Thus, the stoichiometric film 1, with its lattice constant being similar to the pseudocubic one of bulk $La_{0.7}Ca_{0.3}MnO_3$ of 3.864 Å, proves to be nearly free of epitaxial strain. Hence, it contains some lattice defects where the compressive strain imposed by the smaller substrate is relaxed. Oxygen removal results in an increase of the unit cell volume, thereby creating new epitaxial compressive strain in the films and increasing the out-of-plane lattice parameter. None of the x-ray diffractograms showed distinguishable additional peaks that would indicate the presence of a second phase.

In figure 1, the temperature dependence of the resistance, $R(T)$, for the series of oxygen-deficient samples (1 to 7) is shown. (The geometry of measurement is the same for all samples.) The increase of δ leads to an increase of resistivity and a decrease of the metal–insulator transition temperature T_{MI}. The $R(T)$ curves of the samples 4 and 5 show a second peak at a temperature T_2. In the case of sample 6, an overlap of a second resistance peak with the main peak near T_C could be supposed. Sample 7 ($\delta \sim 0.1$) is semiconductive below 80 K. In

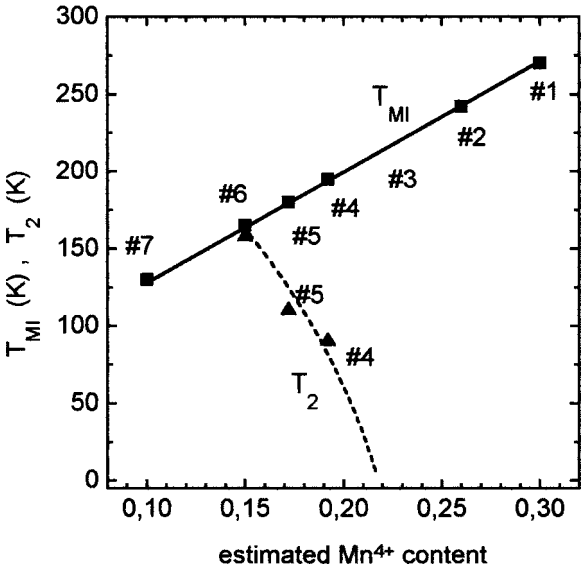

Figure 2. Metal–insulator transition temperature (T_{MI}) and temperature T_2 of the low-temperature resistance peak (see figure 1) plotted in dependence on the approximate Mn^{4+} concentration c of $La_{0.7}Ca_{0.3}MnO_{3-\delta}$ films. The dashed line roughly indicates the T_2 line. No low-temperature peak has been found for an Mn^{4+} content at or above 0.22.

figure 2, T_{MI} and T_2 are plotted versus the estimated Mn^{4+} concentration. The small resistance increase observed for a reoxidized sample (figure 1) is supposed to originate from some structural disorder caused by the diffusion processes. The Curie temperatures (estimated from extrapolation of the linear part of the M^2–T plot to $M = 0$) coincide with T_{MI} within 10 K for all samples. Hence, the oxygen content of the sample *volume* is reduced in the vacuum annealing procedure. The Mn^{4+} contents derived from the values of T_C fit well into a Holstein model description of small-polaron transport for both the present samples and $La_{1-x}Ca_xMnO_3$ [25].

Measurements of the time dependence of resistance were found to be a sensitive tool for detection of small δ changes. Oxygen uptake of oxygen-deficient samples in air has been observed by recording resistance–time curves for several constant temperatures. An example is given in figure 3. The strong decrease of resistance observed at 80 °C is attributed to oxygen diffusion. In other words, the time dependence of the resistance, $R(t)$, is assumed to be due to a time dependence of the oxygen deficiency, $\delta(t)$. Except for a certain time interval at small values of t that belongs to higher values of δ, the $R(t)$ curves can well be fitted to an exponential decay law, $R(t) = R_0(1+\exp(-(t-t_0)/\tau))$, yielding a time constant of $\tau \approx 10^4$ s at 80 °C (inset of figure 3). The sample nearly completely recovered its oxygen content in the course of about 5 hours, with constant resistivity measured after this time. This was also checked by measurement of $R(T)$ in the thus obtained reoxidized state. It becomes clear that efficient oxygen diffusion in our $La_{0.7}Ca_{0.3}MnO_{3-\delta}$ films sets in at a temperature as low as 80 °C. An oxygen uptake at room temperature observed for an insulating oxygen-deficient film (comparable to sample 7) after several weeks led to a metallic state, a second resistance peak near 100 K and an increased T_{MI} (from 130 K to 190 K). Keeping this in mind, our experiments on oxygen-deficient films were done within a few days after preparation.

The temperature dependence of magnetization (figure 4) shows a broadening of the ferromagnetic transitions with increasing δ. These broadened transitions have already been

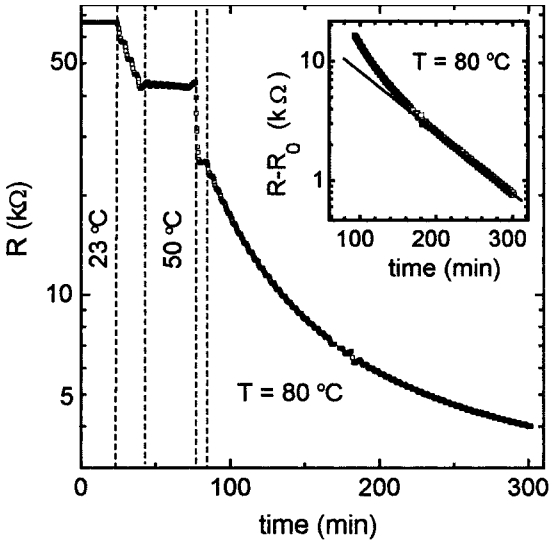

Figure 3. Time dependence of the resistance of an $La_{0.7}Ca_{0.3}MnO_{2.9}$ film in air measured at a temperature of 23 °C, 50 °C and 80 °C, successively. Inset: fit of an exponential law, $R = R_0(1+\exp[-(t-t_0)/\tau])$ (straight line) to the data taken at 80 °C. Fit restricted to $t > 150$ min.

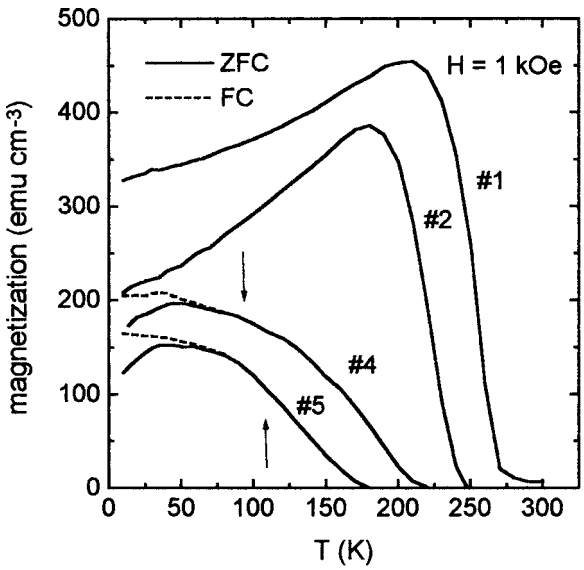

Figure 4. Temperature dependence of magnetization measured in $H = 1$ kOe after zero-field cooling (ZFC) or field cooling in 1 kOe (FC) for some films of figure 1. Arrows mark the temperature T_2 of the low-temperature resistance peak.

observed for oxygen-deficient ceramic samples [10]. On the other hand, the decrease of $M(1;2)$ towards low T is a result of the large saturation field of magnetization at low temperatures, ~5 kOe, in comparison with the field of measurement, 1 kOe. In consistence with the results of figure 4, field-dependent magnetization measurements (not shown here) exhibit a reduction of the spontaneous magnetization $M_S(20\text{ K})$ with increasing δ. For sample 7, M_S has

decreased by about 50% in comparison to sample 1. This is in accordance with findings of [11] for oxygen-deficient ceramic samples and is well known for the low-doping range, $x < 0.3$, of $La_{1-x}Ca_xMnO_3$. The differences between the temperature dependences of the magnetization measured after zero-field cooling (ZFC) or field cooling (FC), respectively (figure 4), point to some kind of spin-freezing behaviour below 50 K. This behaviour, investigated for another Ca-doped manganite and proven to originate from a spin-glass phase [26], was observed for samples 4–7 at low temperatures.

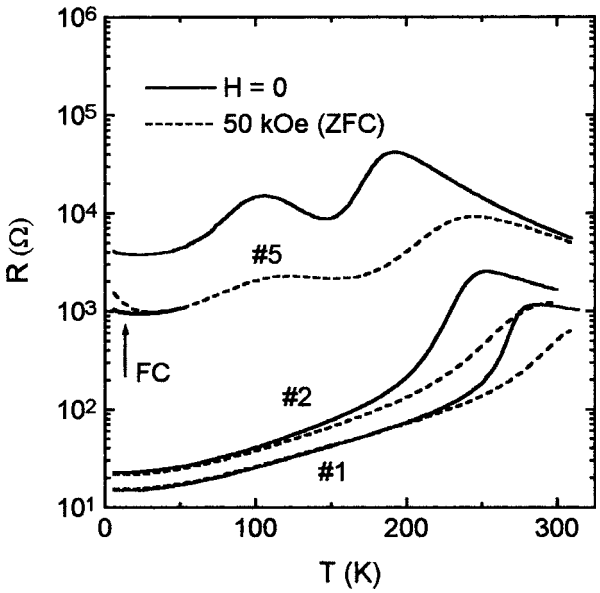

Figure 5. Temperature dependence of resistance measured in magnetic fields of $H = 0$ and 50 kOe after zero-field cooling (ZFC) for some films of figure 1. For sample 5 the low-temperature curve obtained after field cooling (FC) is also shown.

In figures 5 and 6, the temperature dependences of the resistance and the magnetoresistance ratio, MR $= [R(H) - R(0)]/R(0)$, in a magnetic field of $H = 50$ kOe are shown. With increasing oxygen deficiency, the MR peak near T_C is broadened. The magnitude of MR is even somewhat enlarged with increasing δ (figure 6). This is explained by the well known relation of enhancement of CMR when T_C is reduced (e.g. [3]). Higher oxygen deficiency leads to a considerable increase of MR at low temperatures, $T \ll T_C$ (figure 6). A second MR peak is observed near the temperature T_2 of the second resistance peak (e.g. sample 5). In figure 7, the field dependence of MR at 20 K is found to be negligible for the sample without oxygen deficiency (1), while it is strong and hysteretic up to a magnetic field of 50 kOe for the films with high oxygen deficiency. For sample 5, a distinct resistance drop in low magnetic fields, $H < 5$ kOe, can be recognized.

Further indication for spin freezing arises from the difference of low-temperature resistance measured after ZFC or FC, respectively (figure 5). Additionally, the resistance–field curves show a virgin branch remarkably above the cyclic hysteresis loops (figure 7, samples 4 and 5).

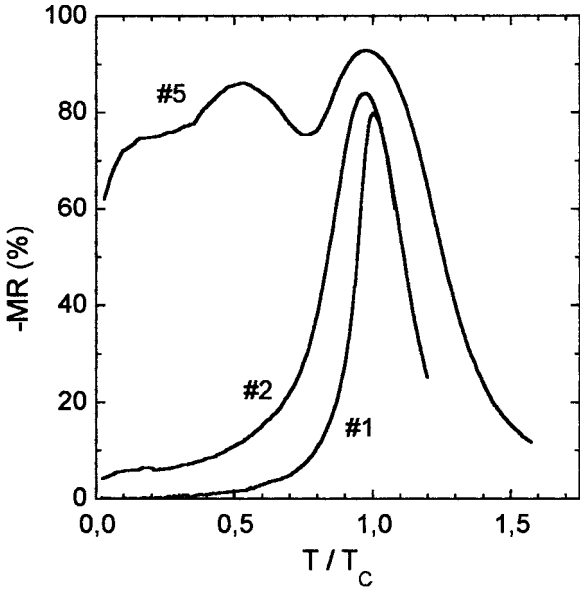

Figure 6. Magnetoresistance ratio, MR $= [R(H) - R(0)]/R(0)$, for $H = 50$ kOe as a function of the reduced temperature T/T_C for the samples of figure 5, based on ZFC measurements.

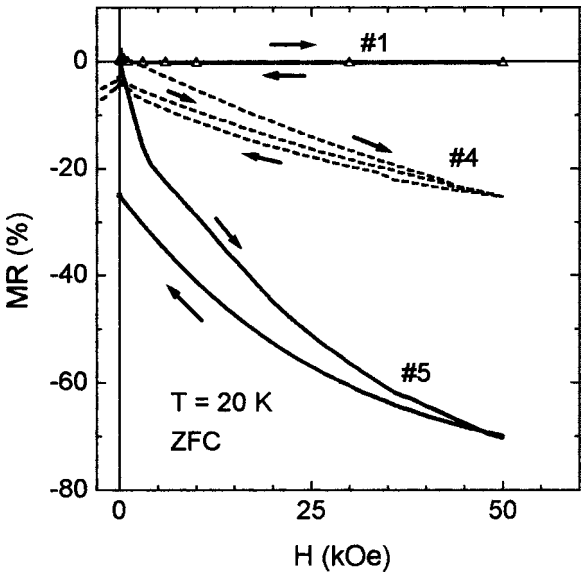

Figure 7. Field dependence of magnetoresistance measured at 20 K after zero-field cooling for some films of figure 1. Arrows indicate the direction of field change.

4. Discussion

From the experimental results shown in figure 3 it becomes clear that efficient oxygen diffusion in $La_{0.7}Ca_{0.3}MnO_3$ thin films, and probably also in other lanthanum manganites, can set in at relatively low temperatures, e.g. as low as 80 °C. As a consequence, oxygen-deficient samples

are highly unstable and difficult to use for technological applications, as e.g. usual lithographic processes take place at higher temperatures. On the other hand, annealing at temperatures much lower than the growth temperature of the films has allowed us to change the oxygen content without change of the film's microstructure. Similarly as in this work, Ju and Krishnan [15] obtained oxygen-deficient $La_{0.7}Sr_{0.3}MnO_{3-\delta}$ films at annealing temperatures of 450 °C to 650 °C, but typically, thin films are annealed at $T \sim 900$ °C in order to control their oxygen content (e.g. [14, 16]). Possibly, fast diffusion along grain boundaries has played a role in our films.

Vacuum annealing was stopped after a certain annealing time, without reaching chemical equilibrium. For this and other reasons, chemical inhomogeneity of the obtained films deserves some consideration. Regions of different oxygen content, and different T_C, could exist within the sample. However, x-ray diffractograms do not indicate *extended* regions of different oxygen content as no additional peaks have been observed and the present $(00n)$ peaks are not extensively broadened with increasing O deficiency. For instance, an extended phase with a T_C as low as the observed temperature of the second resistance peak, T_2 (of 110 K or 90 K), should possess a clearly distinguishable out-of-plane lattice constant. As another source of chemical inhomogeneity, a deviating oxidation state could be present around grain boundaries, if the diffusion length of O for volume diffusion under the used annealing conditions were smaller than the grain diameter [13]. This could result in two transitions in the temperature dependence of resistance [13]. However, for our experiments the interior of the grains seems to be fully included in the O diffusion process since the T_C values derived from magnetization data drop in the same way as the metal–insulator transition temperatures T_{MI} of the deoxygenated films. As a third case, oxygen inhomogeneity could be present within small, some nanometres wide regions that cannot be detected by x-ray diffraction. An example for this has been reported in [12] if certain starting materials had been used for bulk sample preparation. It should be noted that also *intrinsic* clustering of O vacancies may occur as was discussed by Nagaev [21] as an alternative mechanism of phase separation for low-doped manganites.

With respect to the magnetic behaviour the oxygen-deficient films show several indications of *magnetic inhomogeneity* in the sense that they do not consist of a single (maybe canted) ferromagnetic phase. The increasing broadening of $M(T)$ magnetization curves with reduced oxygen content (figure 4) points to a distribution of T_C values in the sample volume. The freezing behaviour obvious in ZFC and FC magnetization–temperature curves resembles that of a spin (cluster) glass or a superparamagnet [11, 26]. The increasing hysteresis of magnetization, $M(H)$, and resistance (figure 7) up to large fields, $H = 50$ kOe, further supports the suggested magnetic inhomogeneity.

In the following it will be shown that the experimental results can be readily discussed in the framework of a magnetic phase diagram including a phase-separated region at low doping that has been suggested recently by von Molnár and Coey [22] (reproduced in figure 8). The temperature dependence of the resistivity that could be expected according to the phase diagram for an intermediate Mn^{4+} content, $c_1 < c(Mn^{4+}) < c_2$ (see figure 8), is as follows. If such a sample is cooled down from the paramagnetic state, the well known metal–insulator transition near T_C and a metallic behaviour below T_C will be observed. Then a phase-separated region is entered at a temperature T_1, that must be characterized by a larger resistivity. Therefore, the second resistance peak found for some of our samples at T_2 is suggested to reflect the transition to a phase separated state. There is a qualitative agreement of the T_1 line in the phase diagram (figure 8) and the measured T_2 values in figure 2. In the two-phase region, electrical conduction would mainly depend on the spatial distribution of the highly conductive ferromagnetic phase. Whether this phase is continuous or mainly consists of separated islands determines the metallic or semiconductive, respectively, nature of the sample, as the antiferromagnetic phase

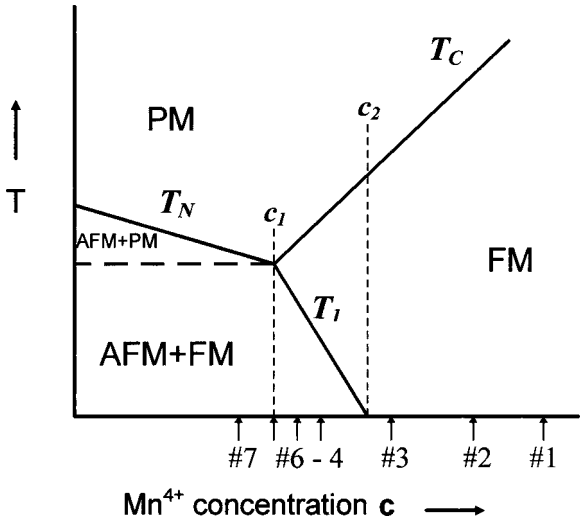

Figure 8. Magnetic ordering temperatures versus Mn^{4+} concentration for low Mn^{4+} concentrations (redrawn after [22]). Abbreviations denote: FM—ferromagnetic, AFM—antiferromagnetic, PM—paramagnetic, T_C—Curie temperature, T_N—Néel temperature, T_1—transition temperature to the area of phase separation. The approximate position of the investigated $La_{0.7}Ca_{0.3}MnO_{3-\delta}$ samples 1–7 is indicated by arrows.

is expected to be semiconductive. According to this picture, sample 7 ($\delta \sim 0.1$) with a semiconductive $R(T)$ dependence (figure 1) and a saturation magnetization reduced by about 50% is suggested to consist of ferromagnetic inclusions in an antiferromagnetic matrix. This is in good agreement with small-angle neutron scattering measurements in a sample with similar Mn^{4+} content, $La_{0.9}Ca_{0.1}MnO_3$ [4].

In the following, the MR behaviour will be discussed. The purely ferromagnetic samples, 1 and 2, show the well known CMR near T_C (figures 5 and 6). They do not exhibit significant MR at $T \ll T_C$, since in well textured films, similar to single crystals, magnetic domain processes produce only a weak MR effect [3]. Within the phase separation picture for the more oxygen-deficient samples, percolation within the ferromagnetic metallic volume fraction is still present for samples 4–6 (figure 1), while sample 7 seems to be beyond the percolation threshold. The application of a magnetic field should slightly increase the ferromagnetic volume fraction. Near the percolation threshold, a small expansion of the ferromagnetic metallic regions can be expected to reduce the resistance considerably. Hence, a large MR could be observed for the two-phase state at low temperatures, as is the case, e.g., for sample 5 (figure 6). Furthermore, near the percolation threshold, ferromagnetic regions are weakly coupled only, resulting in a different direction of magnetization in neighbouring regions [19]. In this case, spin-dependent transport of carriers between adjacent ferromagnetic entities could lead to an MR in lower magnetic fields that is associated with the magnetization process. This mechanism would be similar to the well known grain boundary MR of polycrystalline manganites [3, 10, 24]. Indeed, a distinct MR in low magnetic fields, $H < 5$ kOe, is found for sample 5 (figure 7), that supports this idea.

The grain boundaries being present in the films are less important for the transport properties in the fully oxidized state, but this cannot be expected to be straightforward for the oxygen-deficient state. Two $R(T)$ maxima and a low-field MR at $T < T_C$ have been reported

as a consequence of grain boundary transport between misoriented grains [27]. Though the investigated films are well oriented, the combination of structural defects being present at grain boundaries with the oxygen deficiency could lead to a non-ferromagnetic and highly resistive grain boundary region, while the grains themselves are ferromagnetic and metallic. If only the structurally modified region at grain boundaries is non-ferromagnetic, magnetization of the sample would not be decreased much. For our films, the unusual MR behaviour is associated with a considerably reduced magnetization, thus indicating a minor role of the above described grain boundary effect.

The effect of the tetragonal distortion of the investigated films due to strain resulting from oxygen removal cannot be well separated from the effect of reduced carrier density for the results presented. Oxygen deficiency tends to increase the volume of the unit cell, while the in-plane lattice constants are fixed due to the epitaxy if there is no stress relaxation. Thus, the oxygen-deficient films must be tetragonally distorted since the vacuum treatment was done at rather low temperatures with respect to strain relaxation. The tetragonal distortion, as the Mn–O distance is increased in the film normal, tends to weaken the ferromagnetic double exchange and may have contributed to the observed changes of magnetic (e.g. T_C) and electrical transport (e.g. $R(T)$) properties. Further work should try to compare films on different substrates in order to separate the effects of lattice strain and oxygen stoichiometry.

In conclusion, the magnetic and the resistive behaviour of oxygen-deficient epitaxial $La_{0.7}Ca_{0.3}MnO_{3-\delta}$ thin films prepared by vacuum annealing at intermediate temperatures has been studied. Effective oxygen diffusion in oxygen-deficient films was detected even for $T = 80\,^{\circ}C$ by measurement of the time dependence of resistance, demonstrating the instability of the oxygen-deficient state of manganite thin films. With increasing oxygen deficiency δ, the reduced Mn^{4+} concentration accounts for the observed decrease of the ferromagnetic transition temperature and, at an Mn^{4+} content below (20%, the appearance of a magnetically inhomogeneous state. Our results are consistent with a phase-separated ground state of $La_{0.7}Ca_{0.3}MnO_{3-\delta}$ with less than about 20% Mn^{4+}, that is characterized by the coexistence of ferromagnetic metallic and antiferromagnetic semiconductive regions. The electrical transport in oxygen-deficient films, e.g. the large magnetoresistance in the whole temperature range of $T < T_C$ as well as the low-field magnetoresistance observed for some of the investigated samples, can be explained by a percolation mechanism in the phase-separated state.

Acknowledgments

The authors are grateful to S von Molnár for helpful hints. This work was financially supported by DFG (SFB 422), NATO grant CLG 975357 and a fellowship from the Saxonian Ministry (KD).

References

[1] von Helmolt R, Wecker J, Holzapfel B, Schultz L and Samwer K 1993 *Phys. Rev. Lett.* **71** 2331
[2] Jin S, Tiefel T H, McCormack M, Fastnacht R A, Ramesh R and Chen L H 1994 *Science* **264** 413
[3] Coey J M D, Viret M, and von Molnár S 1999 *Adv. Phys.* **48** 166
[4] Ibarra M R and De Teresa J M 1998 *Giant Magnetoresistance and Related Properties of Metal Oxides* ed C N R Rao and B Raveau (Singapore: World Scientific) pp 83–155
[5] Zener C 1951 *Phys. Rev.* **81** 440
Zener C 1951 *Phys. Rev.* **82** 403
[6] Anderson P W and Hasegawa H 1955 *Phys. Rev.* **100** 675
[7] De Gennes P-G 1960 *Phys. Rev.* **118** 141

[8] Radaelli P G, Iannone G, Marezio M, Hwang H Y, Cheong S-W, Jorgensen J D and Argyriou D N 1997 *Phys. Rev.* B **56** 8265
[9] De Léon-Guevara A M, Berthet P, Berthon J, Millot F and Revcolevschi A 1997 *J. Alloys Compounds* **262/263** 163
[10] Ju H L, Gopalakrishnan J, Peng J L, Qi Li, Xiong G C, Venkatesan T and Greene R L 1995 *Phys. Rev.* B **51** 6143
[11] Ju H L and Sohn H 1997 *J. Magn. Magn. Mater.* **167** 200
[12] Sun J R, Rao G H and Zhang Y Z 1998 *Appl. Phys. Lett.* **72** 3208
[13] Akther Hossain A K M, Cohen L F, Kodenkandeth T, MacManus-Driscoll J and Alford N McN 1999 *J. Magn. Magn. Mater.* **195** 31
[14] Malde N, De Silva P S I P N, Akther Hossain A K M, Cohen L F, Thomas K A, MacManus-Driscoll J L, Mathur N D and Blamire M G 1998 *Solid State Commun.* **105** 643
[15] Ju H L and Krishnan K M 1997 *Solid State Commun.* **104** 419
[16] Panagiotopoulos I, Kallias G, Pissas M, Psycharis V and Niarchos D 1998 *Mater. Sci. Eng.* B **53** 272
[17] Allodi G, De Renzi R, Guidi G, Licci F and Peiper M W 1997 *Phys. Rev.* B **56** 6036
[18] Ibarra M R, Zhao G, De Teresa J M, García-Landa B, Arnold Z, Marquina C, Algarabel P A, Keller H and Ritter C 1998 *Phys. Rev.* B **57** 7446
[19] Uehara M, Mori S, Chen C H and Cheong S-W 1999 *Nature* **399** 560
[20] Yunoki S, Ju H, Malvezzi A L, Moreo A, Furukaw N and Dagotto E 1998 *Phys. Rev. Lett.* **80** 845
[21] Nagaev E L 1996 *Phys. Lett.* A **218** 367
[22] von Molnár S and Coey J M D 1998 *Curr. Opinion Solid State Mater. Sci.* **3** 171
[23] Tranquada J M, Axe J D, Ichikawa N, Moodenbaugh A R, Nakamura Y and Uchida S 1997 *Phys. Rev. Lett.* **78** 338
[24] Vlakhov E S, Chakalov R A, Chakalova R I, Nenkov K A, Dörr K, Handstein A and Müller K-H 1998 *J. Appl. Phys.* **83** 2152
[25] De Teresa J M, Dörr K, Müller K-H, Chakalova R I and Schultz L 1998 *Phys. Rev.* B **58** R5928
[26] De Teresa J M, Ibarra M R, García J, Blasco J, Algarabel P A, Marquina C and Del Moral A 1996 *Phys. Rev. Lett.* **76** 3296
[27] Klein J, Hofener C, Uhlenbruck S, Alff L, Buchner B and Gross R 1999 *Europhys. Lett.* **47** 371